Femtosecond Spectroscopy and Dynamics of the Azulenylosquaric Dye, a Near-infrared Nonfluorogenic Quencher

Yi-Ming Cheng[a] (鄭宜明), I-Che Wu[a] (吳以哲), Chin-Hung Lai[a] (賴金宏), Shih-Chieh Pu[a] (浦士杰), Pi-Tai Chou[a]* (周必泰), Ching-Yen Wei[b]* (衛靖燕), Chao-Ying Yu[b] (余昭穎), Yi-Hsin Lin[b] (林宜心) and Ching Ting[b] (丁　晴)

[a]*Department of Chemistry, National Taiwan University, Taipei 10617, Taiwan, R.O.C.*

[b]*Industrial Technology Research Institute, Hsinchu 30011, Taiwan, R.O.C.*

An azulenylosquaric dye (**ASQ**) has been synthesized to investigate its associated photophysical properties. **ASQ** is essentially nonluminescent ($\Phi_f < 3 \times 10^{-6}$) in any solvent despite its very high absorption extinction coefficient (760 nm, $\varepsilon \sim 8.2 \times 10^4$ $M^{-1}cm^{-1}$ in methanol). Femtosecond fluorescence upconversion, anisotropy kinetics and transient absorption experiments, in combination with the theoretical time-dependent DFT approach, leads us to conclude that the 760 nm absorption is ascribed to the fully allowed $S_0 \rightarrow S_n$ (n 2) transition. The observed < 130 fs decay component is attributed to the $S_n \rightarrow S_1$ internal conversion, while the $S_1 \rightarrow S_0$, with a slower radiative decay time (> 233 ns) undergoes a dominant radiationless deactivation process (710 70 fs) possibly governed by strong interaction between S_1 and S_0 potential energy surfaces.

Keywords: Fluorescence upconversion; Azulenylosquaric dye; Transient absorption; DFT; Internal conversion.

INTRODUCTION

Fluorescent compounds have found numerous useful applications in medicine, biotechnology, and biological science.[1,2] Specifically, fluorochromes attached to various receptors have been used for detecting nucleic acid hybridization (molecular beacons),[3,4] in drug discovery,[5] for sensing molecular interactions,[6,7] and for deciphering biological pathways,[8] etc. In prototypical applications, such as molecular DNA beacons[3,4] and enzyme-sensing probes,[9] the methodology relies on the fluorescence resonance energy transfer (FRET) between a fluorochrome and a quencher. In this approach, highly sensitive, efficient, and quenchable chromophores become essential for acquiring genomic and proteomic information from biological samples.[10] In the visible range, one commonly used quencher to pair with those fluorochromes is, e.g., 4-(4-dimethylaminobenzeneazo) benzoic acid because the majority of sensors fluoresce in the visible light range (< 650 nm).[11]

Recently, chromophores fluorescing in the near-infrared (NIR) range have attracted much attention primarily due to the need for multi-color probes available for simultaneous sensing or encoding,[12,13] as well as the extension of the depth in imaging molecular interactions in vivo.[14-21] As for the corresponding FRET application, the development of efficient, biocompatible, and conjugatable NIR quenchers has become urgent. Recently, a generic type of compound that efficiently quenches NIR fluorescence has been developed by Tung et al.[22] By linking two azulene moieties via a cyclic bridge, Tung et al. have synthesized an azulene-squaric acid coupled dye (**ASQ**, see Scheme I) and successfully demonstrated how derivatives of this model compound can be used for protease sensing in the near-infrared spectrum. The great stability, biocompatibility, and suitability for either solid-phase or aqueous chemistry, in combination with the fine-tuning of the derivatives,[23] have proven its versatility in FRET applications.

Despite its great potential in applications, the fundamental approach of **ASQ** on its associated photophysical properties, unfortunately, is far behind. Considering the remarkably high absorptivity in the lower lying absorption peak of 760 nm ($\varepsilon \sim 8.2 \times 104$ $M^{-1}cm^{-1}$ in methanol), one

Dedicated to the memory of the late Professor Ho Tong-Ing.

* Corresponding author. E-mail: chop@ntu.edu.tw; swei@itri.org.tw

Scheme I Truncated structure of **ASQ** for theoretical approaches

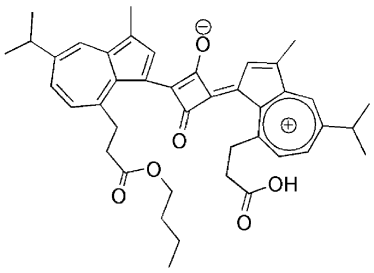

Structure of ASQ

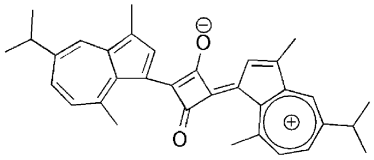

would be surprised at its steady-state nonluminescent property in any solvents as well as at the cryogenic temperature of 77 K (vide infra). Recently, we have initiated an NIR-FRET project using **ASQ** as a quencher in the protease sensing. Being in the field of spectroscopy and dynamics, we feel obliged to shed light on the corresponding photophysics of **ASQ** prior to its bio-applications. Herein, we report the femtosecond fluorescence upconversion and transient absorption, as well as the theoretical approaches of **ASQ**. We believe that the results elaborated as follows should spark a broad spectrum of interest in the relevant research fields.

EXPERIMENTAL SECTION

Materials

ASQ was prepared and purified according to the report by Tung and co-workers.[22] The structure was confirmed based on the following characterization: R_f = 0.34 (9:1 $CHCl_3$/acetone); ^{1}H NMR (300 MHz, $CDCl_3$) 0.78 (t, J = 7.3 Hz, 3H), 1.19 (m, 2H), 1.39 (d, J = 6.7 Hz, 14H), 2.55 (s, 6H), 2.62 (t, J = 7.3 Hz, 2H), 3.11 (m, 4H), 3.90 (t, J = 6.6 Hz, 2H), 4.04 (t, J = 8.0 Hz, 2H), 4.16 (t, J = 7.4 Hz, 2H), 7.63 (m, 4H), 8.13 (s, 2H), 8.78 (s, ^{1}H), 9.01 (s, ^{1}H); ^{13}C NMR (50 MHz, $CDCl_3$) 13.1, 13.6, 19.0, 24.2, 30.5, 34.0, 34.8, 35.8, 36.4, 38.4, 64.6, 121.1, 131.5, 134.4, 138.5, 139.9, 141.8, 148.2, 151.3, 152.6, 154.6, 172.9, 173.7, 178.8, 183.9; HRMS (ES): calcd (M-) ($C_{42}H_{47}O_6$) 647.3372, found 647.3364, UV-vis (methanol) λ_{max} = 758 nm.

Measurement

Steady-state absorption was recorded by a Hitachi (U-3310) spectrophotometer. For the steady-state NIR fluorescence measurement, the fundamental train of pulses (760-820 nm) from Ti-Sapphire oscillator (82 MHz, Spectra Physics) was used as the excitation source. This high-repetition laser beam was treated as a continuous light source and was further chopped by an optical chopper to 134 Hz. The emission was then sent through a lock-in amplifier (Stanford Research System model SR830 DSP) incorporating a 27.5 cm monochromator (ARC SpectraPro-275) equipped with 600 groves/mm gratings blazed at 1.25 m and detected by an NIR sensitive photomultiplier (Hamamatsu model R5509-72) operated at -80 C. A series of holographic filters (Kaiser Optical Systems, Inc.) were used to exclude the excitation laser wavelengths.

Detailed setup of the femtosecond upconversion measurements has been described in a previous report.[24] The reconstruction of time-resolved fluorescence spectra was performed according to a method described previously.[25,26] Briefly, the upconverted emission signal was analyzed by the sum of exponential functions, and consequently renders a temporal resolution of ~150 fs. The deconvoluted emission dynamic data for different wavelengths has been corrected by taking into account the absorption spectra of a set of filter combinations and used to reconstruct emission spectra at different times after excitation. A $\lambda/2$ waveplate was used to rotate the excitation polarization to either parallel $I_{\parallel}(t)$ or perpendicular I (t) components. To study fluorescence anisotropy decay, the time-dependent anisotropy function, r(t), was then calculated using the formula.[27]

$$r(t) = \frac{I_{\parallel}(t) - I\ (t)}{I_{\parallel}(t) + 2I\ (t)}$$

The transient absorption system consisted of a femtosecond Ti-Sapphire oscillator coupled to a regenerative amplifier that generated a ~ 130 fs, 0.3 mJ light pulse (760-830 nm, 1 kHz), which was then split into two beams. One (0.01 mJ) passed through a delay stage and served as an excitation pulse. The major component (0.29 mJ) was then focused into water flowing in a 2 cm cell to generate a white light continuum. Two areas of the sample cell separated vertically by ~ 1 mm were used as the reference and sample parts. Both reference and sample continuum pulses were detected by upper and lower photodiode arrays. The net

change of the absorbance in the "sample" was obtained by taking the logarithm of the ratios of the transmission measured in reference and sample parts. The system response of the transient absorption detecting system has been calibrated by performing a ground-state instantaneous bleaching of sulforhodamine B after excitation at 385 nm as a function of the delay time of the probe pulse at approx. 540 nm.[28] Such an instantaneous rise of the absorption decrease is used to calibrate the delay zero and system response time. The rise time of the system, taking half of the maximum of the bleaching signal, was estimated to be ~ 320 fs, which was then used as a response function in the following fitting process.

RESULTS AND DISCUSSION

Fig. 1 shows the room-temperature absorption and emission spectra of **ASQ** in methanol. The observation of an absorption band maximum at 760 nm with an extinction coefficient of as high as $\varepsilon = 8.2 \times 10^4$ $M^{-1}cm^{-1}$ in methanol suggests the associated transition to be $\pi \rightarrow \pi^*$ in character. The absorbance at the 760 nm peak is linearly proportional to the added **ASQ** concentration from 10^{-7} - 10^{-4} M. This, in combination with the negligible change of the absorption profile, eliminated the possibility of the aggregation effect.

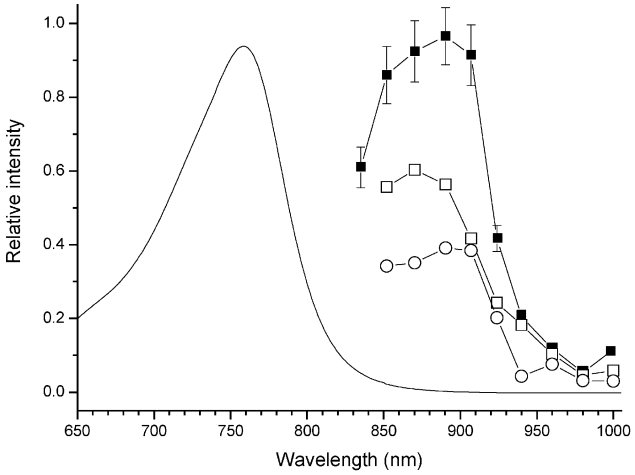

Fig. 1. The absorption spectra (solid line) of **ASQ** in methanol (1.2×10^{-6} M) at 298 K. The corresponding emission spectra (**ASQ**, 1.5×10^{-5} M) acquired from the fluorescence upconversion (λ_{ex} = 760 nm), (■) integration from 0-3 ps, (□) integration at < 3 0 fs (❍) integration from 1-3 ps.

We have also made a major attempt to acquire the associated luminescence. In this approach, the compound bis-(triisobutylsiloxy) silicon-2,3-naphthalocyanine (SiINC) was used as a reference, the 1342 nm phosphorescence yield of which has been determined to be 7×10^{-5} in benzene.[29] Under experimental conditions where the number of photons being absorbed by the **ASQ** and SiINC are identical at, e.g., 760 nm, the best S/N ratio of the SiINC 1340 nm emission was measured to be ~20:1, whereas the attempt to resolve any > 800 nm emission associated with **ASQ** in methanol unfortunately failed even at 77 K. The results also exclude any phosphorescence and hence the possibility of a dominant triplet-state population. We thus determined **ASQ** to be essentially nonluminescent (i.e., emission yield < 3×10^{-6} in methanol). Further details regarding the relationship among quantum yield, radiative decay, and relaxation dynamics are elaborated as follows.

Fig. 2 shows the time-dependent upconverted 890 nm (presumably **ASQ** emission) and 760 nm (pump pulse). The temporal profile seems to consist of two ultrafast decay components. For comparison, an experimental trace of the pump (760 nm) and probe (760 nm) cross-correlation function is also shown in Fig. 2, which gives an fwhm of a

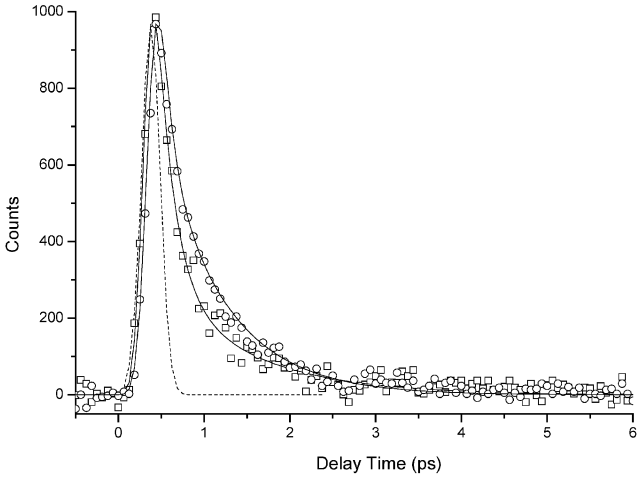

Fig. 2. The time-resolved sum frequency signal of (□) 890 nm (fluorescence) and (❍) 1000 nm (λ_{ex} = 760 nm) for **ASQ** in methanol (1.5×10^{-5} M). The solid lines express the corresponding best-fitted curves. The cross-correlation signal of the 760-nm excitation pulse was also shown here in dashed line. All measurements were performed at 298 K. Fitting for 890 nm: A_1 = 0.715, τ_{f1} = 130 ± 20 fs and A_2 = 0.285, τ_{f2} = 710 70 fs. Fitting for 1000 nm: A_1 = 0.584, τ_{f1} = 150 20 fs and A_2 = 0.416, τ_{f2} = 730 70 fs.

Gaussian shape-like response profile of ~ 130 fs. With the above information provided, we then made an attempt to fit the time-resolved fluorescence intensity ($F(t)$) as a summation of various exponential functions. Incorporating the system response, the fitting equation can be expressed as

$$\sum_{1}^{n}\int_{0}^{t} E(x)i_n(t-x)dx \qquad (1)$$

where $E(x)$ is the system cross-correlation function, n denotes the decay component and $i_n(t\text{-}x)$ is the impulse response function and can be expressed as an exponential term with adjustable amplitude and rate constant. It turned out that the experimental results of **ASQ** could be qualitatively fitted well by two components; one was a system response limited decay component ($\tau_1 < 130$ fs), and the other was resolved to be 710 ± 70 fs. However, the ratio of the pre-exponential factor for < 130 fs versus 710 70 fs components is somewhat dependent on the monitored wavelength, which is ~2.5:1 at 890 nm and then changes to ~1.4:1 at 1000 nm (See Fig. 2 and caption). Upon scanning the monitoring wavelength and integrating the whole decay signals at < 3 ps, an emission profile was resolved and is shown in Fig. 1 with the peak wavelength at 890 nm. However, the spectral temporal evolution monitored at < 300 fs showed a peak wavelength at 870 nm, which was roughly 25 nm blue shifted with respect to that of 895 nm upon integrating the intensity at 1-3 ps. Nevertheless, it is rather difficult to safely differentiate these two spectra due to the poor spectral resolution of ~15 nm and rather small signal-to-noise ratio in the fluorescence upconversion measurement.

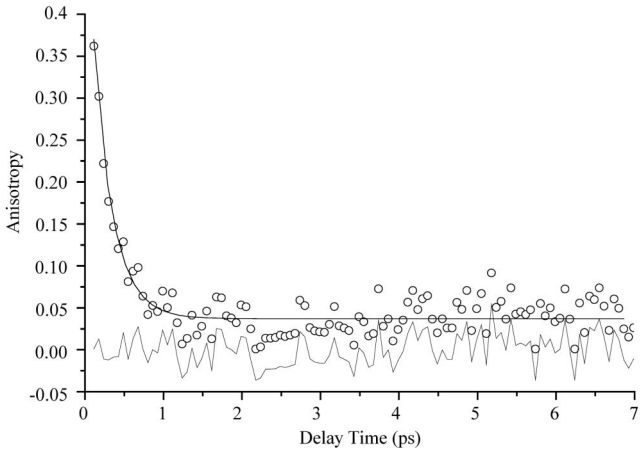

Fig. 3. (Upper) Anisotropy decay constructed from the polarization decay components. The solid line shows the global nonlinear least-squares fit to the data. (bottom) Weighted residuals of the fit.

To gain more insight into the possible states involved in the observed relaxation dynamics we thus performed a fluorescence anisotropy experiment. Fig. 3 shows the global fit of anisotropy decay for **ASQ** monitored at 890 nm. The result revealed an exponential decay constant of r(t), for which the corresponding lifetime was beyond the limit of instrument response time (< 130 fs) and a time-independent constant r(t) value of ~0.05. The results clearly indicate an initial change of direction of the transition moment due to the internal conversion (electronic relaxation), followed by a population decay from the lowest lying excited state, supporting the deactivation pathway of **ASQ** involving at least two low-lying excited states.

Fig. 4 (a) and (b) depict the time-dependent spectral evolution of the transient absorption and the bleaching signal of the $S_0 \rightarrow S_1$ absorption for **ASQ** in methanol at a pump-probe delay time of 0-3 ps. The transient absorption,

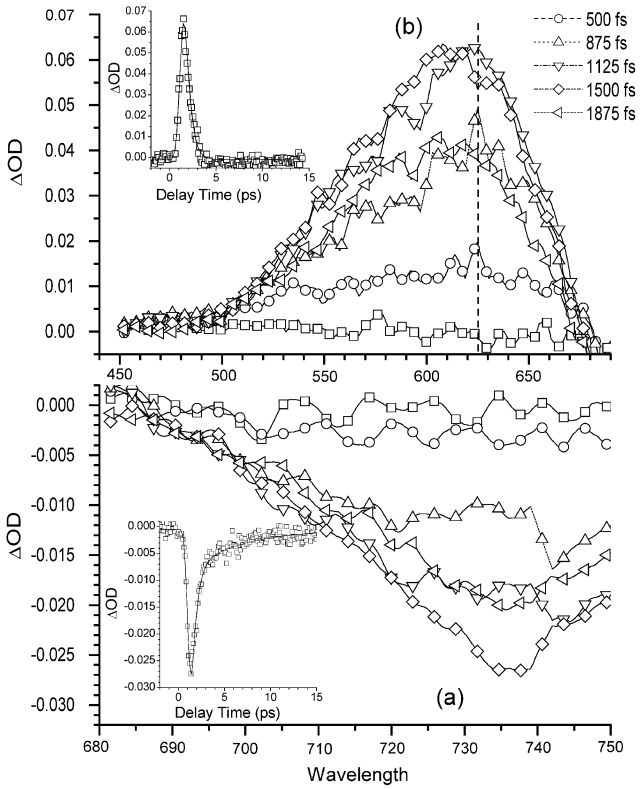

Fig. 4. (a) Transient absorption spectra of **ASQ** in methanol (1.5×10^{-5} M, 298 K) recorded at various time delays between 0.3 and 2 ps after the 760-nm excitation pulse. Insert: Transient absorption kinetics at 600 nm. (b) The bleaching of the **ASQ** ground state. Insert: The bleaching kinetics of **ASQ** at 735 nm.

with peak wavelengths at ~ 600-630 nm, underwent ultrafast fast decay dynamics, with the entire transient absorption profile nearly disappearing after 3 ps. Upon deconvolution with respect to the system response function, the relaxation profile monitored at 600 nm consists of a system response rise (< 320 fs) and a ~ 650 ± 70 fs decay component. Further support of dual decay dynamics is rendered by recovery of the ground state bleaching signal monitored at ~ 735 nm region, being composed of an ultrafast (< 320 fs) and a ~ 680 ± 70 fs decay component similar to that of the transient absorbance data. Note that the difference of peak wavelength from the steady state absorption is possibly attributed to a non-negligible transient absorption band at > 750 nm. This 650 ± 70 fs (or 680 ± 70 fs) decay component, within experimental error, is consistent with that of the 710 ± 70 fs resolved from the fluorescence upconverted signal, respectively. However, the < 130 fs decay component observed in the fluorescence upconversion signal could not be resolved from the transient absorption measurement. This is believed to be mainly due to the relatively slow (~ 320 fs) response time in the transient absorption measurement. One salient feature of the transient profile is that the transient absorption acquired at a delay time of < 500 fs revealed a peak wavelength at ~ 625 nm, which was red shifted by ~ 20 nm with respect to that (~ 605 nm) obtained at a delay time of e.g. > 1.5 ps (see Fig. 4A), indicating the existence of more than one intermediate state to be responsible for the observed spectral profile. Note that the spectral shifts in fluorescence temporal evolution and transient absorption are not continuously evolved. Furthermore, the < 130 fs component resolved from fluorescence upconversion experiments seems much faster than solvent relaxation time of ~7 ps in methanol.[30] As a result, its origin from the solvation relaxation has been devaluated. Unfortunately, due to the sparse solubility and non-luminescent properties of **ASQ** in other organic solvents, further direct proof by applying various solvent polarities and investigating the associated steady state and time-resolved spectroscopy/dynamics could not be performed. Nevertheless, data provided up to this stage lead us to propose a plausible relaxation scheme, in which there exist at least two lower lying states that give rise to the observed relaxation dynamics. We tentatively ascribed these two states as S_1 and S_n states, in which the lowest S_1 state is responsible for the observed slow dynamics, i.e. the ~710 ± 70 fs decay component, and S_n specifies the higher excited state that gives rise to the faster relaxation dynamics of < 130 fs. Under this proposed mechanism, whether the ground absorption peak can be ascribed to the $S_0 \rightarrow S_1$ transition is debatable based on the following experimental evidence.

The radiative decay rate k_r of the S_1 state for **ASQ** has been estimated by Strickler and Bergs' formulation,[31] depicted as

$$k_r = 1/\tau^0 = 2.88x10^{-9} n^2 \left\langle \tilde{\nu}_f^{-3} \right\rangle_{AV}^{-1} \int \frac{\varepsilon(\tilde{\nu}) d\tilde{\nu}}{\tilde{\nu}}$$

where

$$\left\langle \tilde{\nu}_f^{-3} \right\rangle_{AV}^{-1} = \frac{\int F(\tilde{\nu}_f) d\tilde{\nu}_f}{\int \frac{F(\tilde{\nu}_f)}{\tilde{\nu}_f^{-3}} d\tilde{\nu}_f}, \; F(\tilde{\nu}_f)$$

denotes the normalized fluorescence intensity as a function of the wavenumber, and n is the index of refraction for solvents, which is 1.56 in methanol. Assuming the whole integrated area of the 760 nm band to be the S_1 band, k_r for the $S_1 \rightarrow S_0$ transition of **ASQ** was calculated to be $9.9 \times 10^7 s^{-1}$. Note that this result may only be treated as an approximation where the possibility of an overlap between S_1 and other highly electronically excited states has been neglected. In order to explain the Φ_f of $< 3 \times 10^{-6}$, the observed decay rate is deduced to be 3.3×10^{13} s^{-1}, corresponding to a lifetime of < 30 fs, which is much shorter than the observed 710 ± 70 fs decay time in methanol. In order to fit the observed 710 ± 70 fs decay time with Φ_f of $< 3 \times 10^{-6}$, the radiative decay rate was estimated to be $< 4.3 \times 10^6$ s^{-1}, i.e., $\tau_r > 233$ ns). We thus tentatively propose that there exists the lowest lying singlet state (i.e. the S_1 state) with an energy lower than the observed 760 nm (13157 cm^{-1}) band in **ASQ**. Due to its much longer radiative decay time and hence the partially allowed $S_1 \rightarrow S_0$ transition, the associated absorptivity must be rather small and hidden under the allowed 760 nm transition band. Further support of this viewpoint is given by the theoretical approaches described as follows.

Theoretical confirmation of the underlying basis for the photophysical properties of **ASQ** was provided by the *ab initio* MO and time dependent DFT (TDDFT) calculations.[32] Note that due to the structural complexity, a truncated **ASQ** structure (see Scheme I), in which the carboxylic and carboxylate side chains have been reduced to a methyl group, has been adopted for the theoretical approach. Since these side chains are singly bonded with azulene chromophores, their influence on the ππ* transi-

Table 1. The calculated excitation energies, oscillator strengths and the correlated frontier orbitals for **ASQ** (TD-B3LYP/6-31G*//B3LYP/6-31G*)

State	Excitation	E_{cal}, eV	$\ddot{e}_{cal}$, nm	*F*
1	HOMO → LUMO (+48%) HOMO-1 → LUMO (40%)	1.44	860.7	0.0113
2	HOMO-2 → LUMO (+87%)	1.84	673.0	0.0687
3	HOMO → LUMO+1 (+60%) HOMO-1 → LUMO+1 (+30%)	1.89	655.4	0.0232
4	HOMO-1 → LUMO (+32%) HOMO → LUMO (+22%) HOMO-2 → LUMO (8%)	2.05	605.8	1.0895

tion is expected to be rather small. The results for the **ASQ** analogue are shown in Figs. 5, 6 and Table 1. Fig. 5 shows the optimized structure and the charge distributions of **ASQ**. Fig. 6 depicts the features of the two lowest unoccupied (LUMO and LUMO+1) and the two highest occupied (HOMO and HOMO-1) frontier orbitals, mainly involved in the lower-lying transition, while the descriptions and the energy gap of each transition are listed in Table 1. Apparently, the electron densities of the singlet states for both the HOMO and HOMO-1 are located largely on the central squaric acid ring and one side of the azulene moieties, whereas those of the LUMO and LUMO+1 are distributed to the whole molecular framework; this indicates that the lowest electronic transition is dominated by a ππ* character. Furthermore, according to the oscillator strength of < 0.06 calculated by TDDFT, the transitions from S_0 to the first three low lying electronic states (S_1 - S_3) were reasonably considered as a partial allowed process with respect to the fully allowed S_4 state, which possesses an oscillator strength of ~ 1.0. Thus, to our viewpoint, the strong $S_1 \rightarrow S_4$ transition (~ 605 nm) may correlate with the strong 760 nm absorption band with a peak (760 nm) extinction coeffi-

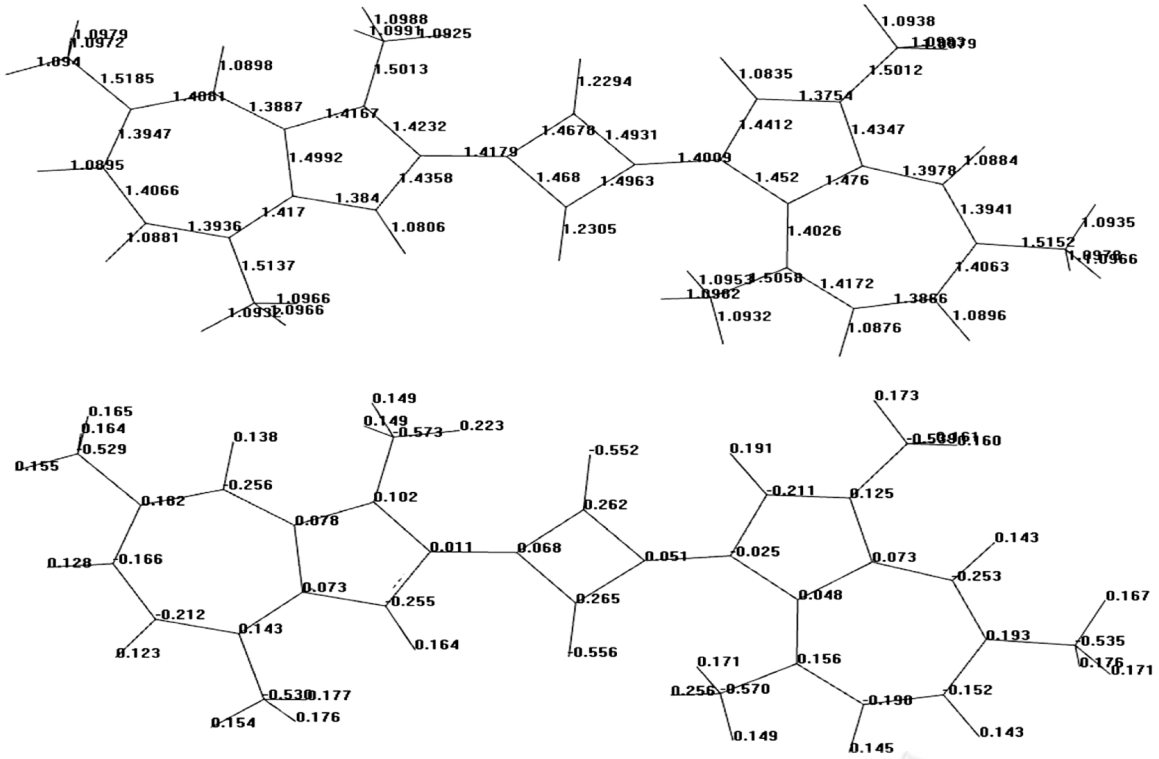

Fig. 5. The optimized structure (upper) and the charge distributions (bottom) of **ASQ**.

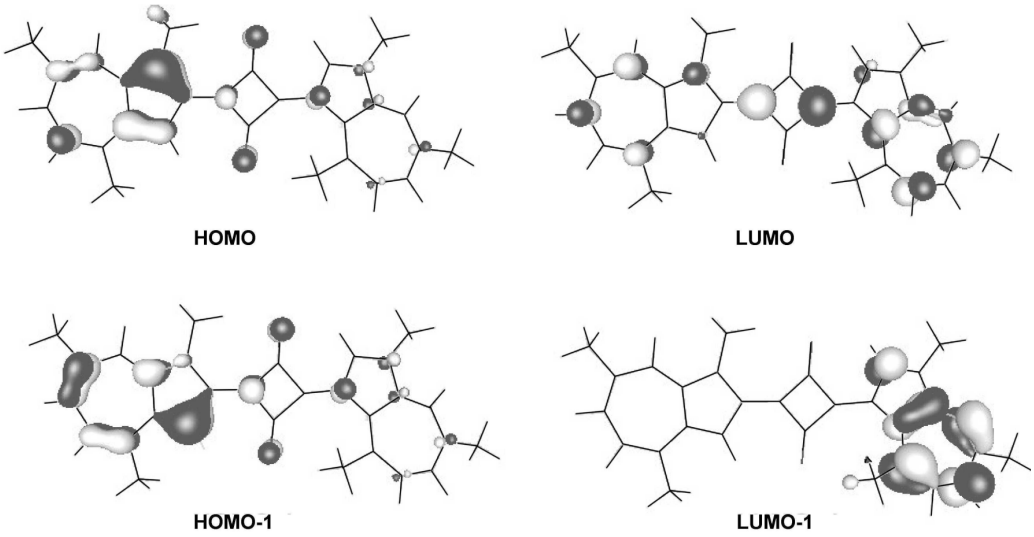

Fig. 6. The calculated frontier molecular orbitals of **ASQ**.

cient of 8.2×10^4 $M^{-1}cm^{-1}$ in methanol. The deviation of the current theoretical approach from the experimental result may plausibly be explained by the absence of the solvation effect in the gas phase. Note that due to the zwitterionic properties in **ASQ**, solvent perturbation is expected to be sensitive to the transition, particularly to the fully allowed transition (760 nm) band. Furthermore, the theoretical level adopted here (i.e. 6-31G* in basis set) may only be suitable for describing photophysical properties of **ASQ** in a qualitative manner. However, the result that the 760 nm absorption band should correlate with a highly electronic excited state is consistent with the experimental observation. On both experimental and theoretical bases, we thus tentatively propose a relaxation pathway of **ASQ** as depicted in Scheme II. Upon a 760-800 nm allowed Franck-Condon excitation, **ASQ** is populated at a highly electronic state of S_n (n~ 4). Subsequently, the S_n-S_1 internal conversion takes place within a time scale of $\leq$ 130 fs. The S_1 state, according to the calculation, should lie in an energy level of ~ 860 nm (11,600 cm^{-1}) with a partial allowed transition in character versus the S_0 state.

Finally, for the fast $S_1 \rightarrow S_0$ deactivation process, as an empirical approach, in the absence of a Zero-Order surface crossing between S_1 and S_0 states (i.e. the match type), the rate constant of a $S_1 \rightarrow S_0$ internal conversion can be estimated by $\nu\exp(-\alpha\Delta E)$ where α is a proportionality constant (~0.18), and the value of ν is taken to be ~$10^{13}s^{-1}$. ΔE is taken to be 32 kcal/mol (~ 900 nm for the emission peak wavelength). Accordingly, the radiationless decay rate

Scheme II The proposed relaxation dynamics of **ASQ** in methanol upon 760-800 excitation. Note that the energy gaps between these electronic states are depicted according to the theoretical result, which should be viewed only as a qualitative approach

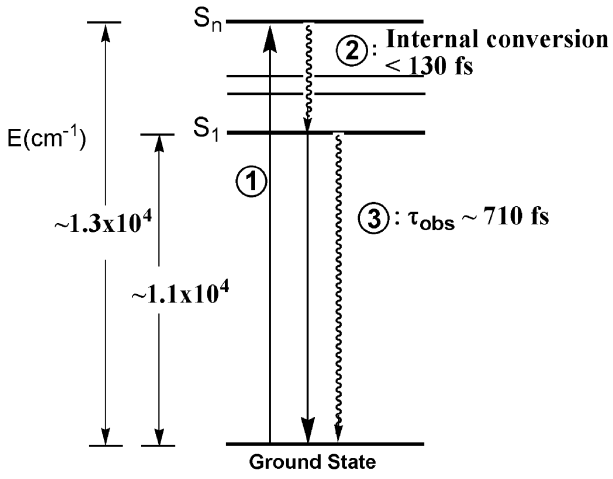

constant of ~3.1×10^{10} s^{-1} estimated from the energy gap law[33] seems to be much smaller than the ~1.4×10^{12} s^{-1} obtained experimentally. Therefore, the unusually short lifetime (~ 710 fs) suggests that the relaxation process may not be governed by a matching mechanism (energy gap law), but instead is dominated by the interaction between S_0 and S_1 states, i.e. a type of crossing mechanism,[34] possibly as-

sociated with the squaric 4-member ring motion. Unfortunately, due to such a complicated molecular structure like azulenylocyanine, the actual large amplitude motion that realizes the zero-order level crossing between S_1 and S_0 states is still pending for resolution.

CONCLUSION

In conclusion, the photophysics of **ASQ** have been investigated by steady state, femtosecond fluorescence upconversion, anisotropy kinetics and transient absorption approaches. The results show an ultrafast rate (< 130 fs^{-1}) of $S_n \rightarrow S_1$ internal conversion (n ~ 4), followed by a fast, radiationless dominated rate (~ 0.7 ps^{-1}) of $S_1 \rightarrow S_0$ relaxation. This, in combination with a long $S_1 \rightarrow S_0$ radiative decay time, gives rise to an essentially non-luminescent property in any solvent. Since the lower lying states are calculated to be close in energy for **ASQ** (see Table 1), it will be very interesting to examine if S_1 and the fully allowed states (e.g. S_4) can be converted through the derivatization of **ASQ**. This approach is rather feasible, since the chemical reactivity of azulene has been studied extensively.[35-38] Thus, absorbance of derivatives may be fine-tuned by replacing the substituents on the azulene rings.[23] For this case, tuning the azulenylocyanines from non-luminescent to luminescent properties may be feasible, the results of which should greatly extend the future FRET applications based on **ASQ** analogues.

ACKNOWLEDGMENT

This work was supported by the National Science Council, Taiwan R.O.C. (Grant NSC 89-2113-M-194-022) and National Center for High Performance Computing.

Received October 13, 2006.

REFERENCES

1. Lakowicz, J. R. *Principles of Fluorescence Spectroscopy*; Plenum Press: New York, 1999.
2. Mitchell, P. *Nat. Biotechnol*. **2001**, *19*, 1013.
3. Sokol, D. L.; Zhang, X.; Lu, P.; Gewirtz, A. M. *Proc. Natl. Acad. Sci. USA*, **1998**, *95*, 11538.
4. Tyagi, S.; Kramer, F. R. *Nat. Biotechnol*. **1998**, *14*, 303.
5. Harris, J. L.; Alper, P. B.; Li, J.; Rechsteiner, M.; Backes, B. J. *Chem. Biol.* **2001**, *8*, 1131.
6. Zlokarnik, G.; Negulescu, P. A.; Knapp, T. E.; Mere, L.; Burres, N.; Feng, L.; Whitney, M.; Roemer, K.; Tsien, R. Y. *Science* **1998**, *279*, 84.
7. Zaccolo, M.; De Giorgi, F.; Cho, C. Y.; Feng, L.; Knapp, T.; Negulescu, P. A.; Taylor, S. S.; Tsien, R. Y.; Pozzan, T. *Nat. Cell Biol.* **2000**, *2*, 25.
8. Zaccolo, M.; Pozzan, T. *IUBMB Life* **2000**, *49*, 375.
9. Wang, G. T.; Matayoshi, E.; Huffaker, H. J.; Krafft, G. A. *Tetrahedron Lett*. **1990**, *31*, 6493.
10. Beaucage, S. L. *Curr. Med. Chem.* **2001**, *8*, 1213.
11. Chan, W. C.; Maxwell, D. J.; Gao, X.; Bailey, R. E.; Han, M.; Nie, S. *Curr. Opin. Biotechnol.* **2002**, *13*, 40.
12. Klein, P. E.; Klein, R. R.; Cartinhour, S. W.; Ulanch, P. E.; Dong, J.; Obert, J. A.; Morishige, D. T.; Schlueter, S. D.; Childs, K. L.; Ale, M.; Mullet, J. E. *Genome Res*. **2000**, *10*, 789.
13. Tong, A. K.; Li, Z.; Jones, G. S.; Russo, J. J.; Ju, J. *Nat. Biotechnol.* **2001**, *19*, 756.
14. Weissleder, R.; Tung, C.-H.; Mahmood, U.; Bogdanov, A. *Nat. Biotechnol.* **1999**, *17*, 375.
15. Tung, C.-H.; Bredow, S.; Mahmood, U.; Weissleder, R. *Bioconjugate Chem.* **1999**, *10*, 892.
16. Bremer, C.; Bredow, S.; Mahmood, U.; Weissleder, R.; Tung, C.-H. *Radiology* **2001**, *221*, 523.
17. Tung, C.-H.; Mahmood, U.; Bredow, S.; Weissleder, R. *Cancer Res*. **2000**, *60*, 4953.
18. Marten, K.; Bremer, C.; Khazaie, K.; Sameni, M.; Sloane, B.; Tung, C.-H.; Weissleder, R. *Gastroenterology* **2002**, *122*, 406.
19. Bremer, C.; Tung, C.-H.; Weissleder, R. *Nat. Med.* **2001**, *7*, 743.
20. Licha, K.; Hessenius, C.; Becker, A.; Henklein, P.; Bauer, M.; Wisniewski, S. Wiedenmann, B. Semmler, W. *Bioconjugate Chem.* **2001**, *12*, 44.
21. Achilefu, S.; Dorshow, R. B.; Bugaj, J. E.; Rajagopalan, R. *Invest. Radiol.* **2000**, *35*, 479.
22. Pham, W.; Weissleder, R.; Tung, C.-H. *Angew. Chem. Int. Ed*. **2002**, *41*, 3659.
23. Pham, W.; Weissleder, R.; Tung, C.-H. *Tetrahedron Lett.* **2002**, *43*, 19.
24. Chou, P. T.; Yu, W. S.; Cheng, Y. M.; Pu, S. C.; Yu, Y. C.; Lin, Y. C.; Huang, C. H.; Chen, C. T. *J. Phys. Chem. A.* **2004**, *108*, 6487.
25. Jarzeba, W.; Walker, G. C.; Johnson, M. A.; Barbara, P. F. *J. Phys. Chem.* **1988**, *92*, 7039.
26. Barbara, P. F.; Jarzeba, W. *Advances in Photochemistry*

1990, *15*, 1.
27. Lakowicz, J. R. *Principles of Fluorescence Spectroscopy*; 2nd ed.; Kluwer Academic/Plenum Publishers: New York, 1999.
28. Elsaesser, T.; Kaiser, W. *Ann. Rev. Phys. Chem.* **1991**, *42*, 83.
29. Chou, P. T.; Chen, Y. C.; Chen, S. J.; Lee, M. J.; Wei, C. Y.; Wen, T. C. *J. Chin. Chem. Soc.* **1998**, *45*, 503.
30. Liu, J.-Y.; Fan, W.-H.; Han, K.-L.; Deng, W.-Q.; Xu, D.-L.; Lou, N.-Q. *J. Phys. Chem. A.* **2003**, *107*, 10857.
31. Strickler, S. J.; Berg, R. A. *J. Chem. Phys.* **1962**, *37*, 814.
32. Casida, M. E. Time-Dependent Density Functional Response Theory of Molecular Systems: Theory, Computational Methods, and Functionals. In *Recent Developments and Applications of Modern Density Functional Theory*; Seminario, J. M., Ed.; Elsevier: Amsterdam, 1996; p 391.
33. Siebrand, W. *J. Chem. Phys.* **1967**, *47*, 2411.
34. Ippen, E. P.; Shank, C. V.; Woerner, R. L. *Chem. Phys. Lett.* **1977**, *46*, 20.
35. Tomiyama, T.; Yokota, M.; Wakabayashi, S.; Kosakai, K.; Yanagisawa, T. *J. Med. Chem.* **1993**, *36*, 791.
36. Ito, S.; Fujita, M.; Morita, N.; Asao, T. *Bull. Chem. Soc. Jpn.* **1995**, *68*, 3611.
37. Chen, S. L.; Klein, R.; Hafner, K. *Eur. J. Org. Chem.* **1998**, 423.
38. Ito, S.; Morita, N.; Asao, T. *Bull. Chem. Soc. Jpn.* **1999**, *72*, 2543.